

## ARTICLE

# Efficient detection of human circulating tumor cells without significant production of false-positive cells by a novel conditionally replicating adenovirus

Fuminori Sakurai<sup>1,2</sup>, Nobuhiro Narii<sup>1</sup>, Kyoko Tomita<sup>1</sup>, Shinsaku Togo<sup>3</sup>, Kazuhisa Takahashi<sup>3</sup>, Mitsuhiro Machitani<sup>1</sup>, Masashi Tachibana<sup>1</sup>, Masaaki Ouchi<sup>4</sup>, Nobuyoshi Katagiri<sup>4</sup>, Yasuo Urata<sup>4</sup>, Toshiyoshi Fujiwara<sup>5</sup> and Hiroyuki Mizuguchi<sup>1,6,7,8</sup>

Circulating tumor cells (CTCs) are promising biomarkers in several cancers, and thus methods and apparatuses for their detection and quantification in the blood have been actively pursued. A novel CTC detection system using a green fluorescence protein (GFP)-expressing conditionally replicating adenovirus (Ad) (rAd-GFP) was recently developed; however, there is concern about the production of false-positive cells (GFP-positive normal blood cells) when using rAd-GFP, particularly at high titers. In addition, CTCs lacking or expressing low levels of coxsackievirus-adenovirus receptor (CAR) cannot be detected by rAd-GFP, because rAd-GFP is constructed based on Ad serotype 5, which recognizes CAR. In order to suppress the production of false-positive cells, sequences perfectly complementary to blood cell-specific microRNA, miR-142-3p, were incorporated into the 3'-untranslated region of the E1B and GFP genes. In addition, the fiber protein was replaced with that of Ad serotype 35, which recognizes human CD46, creating rAdF35-142T-GFP. rAdF35-142T-GFP efficiently labeled not only CAR-positive tumor cells but also CAR-negative tumor cells with GFP. The numbers of false-positive cells were dramatically lower for rAdF35-142T-GFP than for rAd-GFP. CTCs in the blood of cancer patients were detected by rAdF35-142T-GFP with a large reduction in false-positive cells.

*Molecular Therapy — Methods & Clinical Development* (2016) **3**, 16001; doi:10.1038/mtm.2016.1; published online 2 March 2016

## INTRODUCTION

Recently, much attention has been focused on circulating tumor cells (CTCs), which are defined as tumor cells shed from either the primary tumor or its metastases and circulating in the peripheral blood of cancer patients, as a prognostic factor and/or a surrogate biomarker, because it is becoming clear that the number and change in the number of CTCs can be used to evaluate the action of drugs on tumors and is prognostic for progression-free and overall survival in several types of cancer.<sup>1,2</sup> Characterization of CTCs is also expected to enhance understanding of the biology of metastasis.<sup>3,4</sup> However, CTCs are rare, with numbers as low as one CTC in 10<sup>6</sup>–10<sup>7</sup> leukocytes. Although several methods and apparatuses for detection of CTCs have been developed,<sup>5,6</sup> there are several problems with the conventional CTC detection methods. For example, in the CellSearch™ system, which was approved by the US Food and Drug Administration in 2004, CTCs are concentrated using anti-CD45 antibody and anti-epithelial cell adhesion molecule (EpCAM) antibody

and are detected by immunostaining using anti-cytokeratin (CK)-8, anti-CK-9, and anti-CK-19 antibodies; however, these antigens are also expressed on normal epithelial cells. In addition, several types of tumor cells are negative for EpCAM or these CK molecules. Previous studies demonstrated that EpCAM expression levels on CTCs were highly variable and that CTCs expressing low or negligible levels of EpCAM were found in the blood of cancer patients.<sup>7–9</sup>

In order to efficiently and accurately detect and quantify the CTCs in blood, a novel CTC detection method using a green fluorescence protein (GFP)-expressing conditionally replicating adenovirus (Ad) (rAd-GFP; TelomeScan) has been developed.<sup>10,11</sup> rAd-GFP possesses a human telomerase reverse transcriptase (hTERT) promoter-driven E1 gene expression cassette and a GFP expression cassette in the E1- and E3-deleted region of the Ad genome, respectively.<sup>12</sup> Incubation of rAd-GFP with blood cells containing CTCs results in efficient labeling of CTCs with GFP, because rAd-GFP efficiently replicates in an hTERT-positive cell-specific

The first three authors contributed equally to this work.

<sup>1</sup>Laboratory of Biochemistry and Molecular Biology, Graduate School of Pharmaceutical Sciences, Osaka University, Osaka, Japan; <sup>2</sup>Laboratory of Regulatory Sciences for Oligonucleotide Therapeutics, Clinical Drug Development Unit, Graduate School of Pharmaceutical Sciences, Osaka University, Osaka, Japan; <sup>3</sup>Division of Respiratory Medicine, Juntendo University Faculty of Medicine & Graduate School of Medicine, Tokyo, Japan; <sup>4</sup>Oncology Biopharma, Tokyo, Japan; <sup>5</sup>Department of Gastroenterological Surgery, Okayama University Graduate School of Medicine, Dentistry and Pharmaceutical Sciences, Okayama, Japan; <sup>6</sup>The Center for Advanced Medical Engineering and Informatics, Osaka University, Osaka, Japan; <sup>7</sup>Laboratory of Hepatocyte Differentiation, National Institute of Biomedical Innovation, Osaka, Japan; <sup>8</sup>iPS Cell-Based Research Project on Hepatic Toxicity and Metabolism, Graduate School of Pharmaceutical Sciences, Osaka University, Osaka, Japan. Correspondence: F Sakurai (sakurai@phs.osaka-u.ac.jp) Or H Mizuguchi (mizuguch@phs.osaka-u.ac.jp)

Received 22 June 2015; accepted 25 November 2015

manner, leading to efficient expression of GFP in CTCs. Expression levels of hTERT are upregulated in most tumor cells. This method detected the tumor cells spiked in the blood more sensitively than real-time RT-PCR-based method. In order to correctly and efficiently detect CTCs by rAd-GFP, combinational use of infection with rAd-GFP and immunostaining with antibodies, including anti-CD45 antibody, is preferable. Although, ideally, high titers of rAd-GFP would be used to efficiently detect CTCs, large numbers of false-positive cells (GFP-expressing normal blood cells) are observed following infection with high titers of rAd-GFP. In addition, although immunostaining with anti-CD45 antibody is a promising method to rule out GFP-expressing normal blood cells, perfect immunostaining of all of the normal blood cells in samples might not be possible due to the extremely large numbers of blood cells in the samples, which would increase the chances for the production of false-positive cells. In order to efficiently detect CTCs but prevent the production of false-positive cells as much as possible when using conditionally replicating Ads, we incorporated four copies of a sequence perfectly complementary to blood cell-specific microRNA (miRNA), miR-142-3p,<sup>13</sup> into the 3'-untranslated region (3'-UTR) of both the E1 and GFP genes. While most CTCs would express extremely low or undetectable levels of miR-142-3p, blood cells express miR-142-3p at high levels. A previous study demonstrated that miR-142-3p expression in the CTCs of breast cancer patients was much lower than that in normal leukocytes.<sup>14</sup> We hypothesized that expression of the E1 and GFP genes is efficiently suppressed at the post-transcriptional level in a blood cell-specific manner by incorporation of miR-142-3p complementary sequences in the 3'-UTR of these genes, leading to the reduction in the number of false-positive cells.

There is another drawback to the CTC detection method using rAd-GFP. CTCs lacking or expressing low levels of coxsackievirus-adenovirus receptor (CAR) cannot be efficiently detected by rAd-GFP. rAd-GFP is constructed based on Ad serotype 5 (Ad5), which recognizes CAR as an infection receptor. CAR-positive CTCs are efficiently labeled with GFP by rAd-GFP; however, rAd-GFP is not able to efficiently mediate GFP expression in CAR-negative CTCs. Unfortunately, it is expected that CAR expression on CTCs will often be low because malignant metastatic tumor cells and tumor cells undergoing epithelial-mesenchymal transition (EMT) often show low or negligible levels of CAR expression.<sup>15,16</sup> CTCs are well correlated with tumor metastasis and are often undergoing EMT.<sup>17</sup> Therefore, in order to overcome the problem described above, the fiber protein of rAd-GFP was substituted with that of Ad serotype 35 (Ad35). Ad35 recognizes human CD46,<sup>18</sup> which is ubiquitously expressed on almost all human cells, including CAR-negative tumor cells, as an infection receptor. Moreover, CD46 expression has been demonstrated to be upregulated on malignant tumor cells.<sup>19,20</sup> CAR-negative CTCs would be efficiently infected with a conditionally replicating Ad possessing Ad35 fiber protein.

In this study, we developed a novel conditionally replicating Ad (rAdF35-142T-GFP) for detection of both CAR-positive and CAR-negative CTCs without production of false-positive cells. rAdF35-142T-GFP possesses the fiber protein of Ad35. miR-142-3p complementary sequences were inserted into the 3'-UTR of the E1 and GFP genes in the Ad genome. The number of false-positive cells was dramatically reduced by use of rAdF35-142T-GFP, compared with rAd-GFP. rAdF35-142T-GFP efficiently mediated GFP expression in both CAR-positive and CAR-negative tumor cells. CTCs in the blood of cancer patients were detected by rAdF35-142T-GFP without significant production of false-positive cells.

## RESULTS

Development of a conditionally replicating Ad containing Ad35 fiber protein and the miR-142-3p-regulated gene expression system

In order to suppress the production of false-positive cells and to efficiently detect both CAR-positive and CAR-negative CTCs, the following modifications were introduced into rAd-GFP, producing rAdF35-142T-GFP (Figure 1, Supplementary Table S1). First, the fiber proteins of rAd-GFP were replaced with those derived from Ad35. We previously demonstrated that a replication-incompetent Ad vector possessing fiber protein of Ad35 efficiently transduces not only CAR-positive cells but also CAR-negative cells,<sup>21,22</sup> indicating that both CAR-positive and CAR-negative CTCs are susceptible to a conditionally replicating Ad possessing Ad35 fiber protein. Second, four copies of sequences perfectly complementary to miR-142-3p, which is specifically expressed in blood cells, were incorporated into the 3'-UTR of both the E1B and GFP genes. We hypothesized that incorporation of miR-142-3p-targeted sequences into the 3'-UTR of the E1B and GFP genes resulted in the suppression of the E1 and GFP gene expression in a blood cell-specific manner, leading to a reduction in the production of false-positive cells. rAdF35-142T-GFP was produced using H1299 cells, which is a human non-small-cell lung carcinoma cell line highly susceptible to oncolytic Ads,<sup>23</sup> as a packaging cell, instead of 293 cells, in order to avoid homologous between the genome of the conditionally replicating Ad genome and the Ad gene in the 293 cell genome. We also created rAdF35-GFP, in which fiber protein of Ad35, not miR-142-3p-targeted sequences, was introduced into rAd-GFP, as a control conditionally replicating Ad.

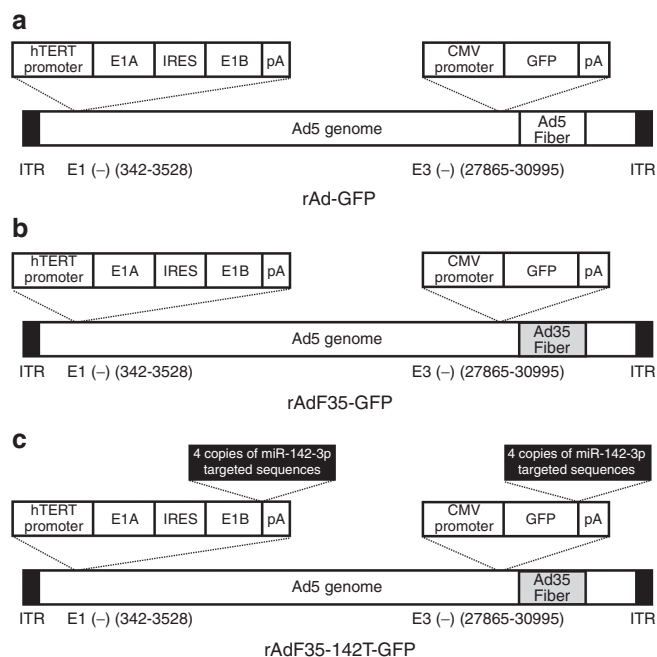


**Figure 1** Schematic diagram of conditionally replicating Ads used in this study. (a) rAd-GFP, (b) rAdF35-GFP, and (c) rAdF35-142T-GFP. rAdF35-GFP was developed by replacing the fiber protein of rAd-GFP with Ad35 fiber protein. rAdF35-142T-GFP was developed by inserting miR-142-3p-targeted sequences into the 3'-UTR of both the E1 gene and GFP gene of rAdF35-GFP. CMV, cytomegalovirus; GFP, green fluorescence protein; hTERT, human telomerase reverse transcriptase; IRES, internal ribosomal entry site; ITR, internal terminal repeat; pA, bovine growth hormone polyadenylation signal; UTR, untranslated region.

Expression levels of CAR, CD46, hTERT, and miR-142-3p in cultured tumor cell lines and PBMCs

Next, in order to examine the expression levels of CAR and CD46 on the cultured tumor cells and peripheral blood mononuclear cells (PBMCs), flow cytometric analysis was performed. Although most of the tumor cell lines examined were CAR positive, the CAR expression levels were extremely low or were not detectable on T24, LNZ308, LN444, and K562 cells (Figure 2a). MCF7, MDA-MB-231,

and PANC-1 cells expressed intermediate levels of CAR. On the other hand, all of the human tumor cell lines examined, except for SF295 cells, highly expressed human CD46. CD46 was not detectable on SF295 cells. We previously demonstrated that human PBMCs highly expressed CD46.<sup>24</sup>

miR-142-3p and hTERT expression levels were evaluated by real-time RT-PCR analysis. PBMCs and K562 cells expressed approximately 100-fold higher levels of miR-142-3p than the other adherent

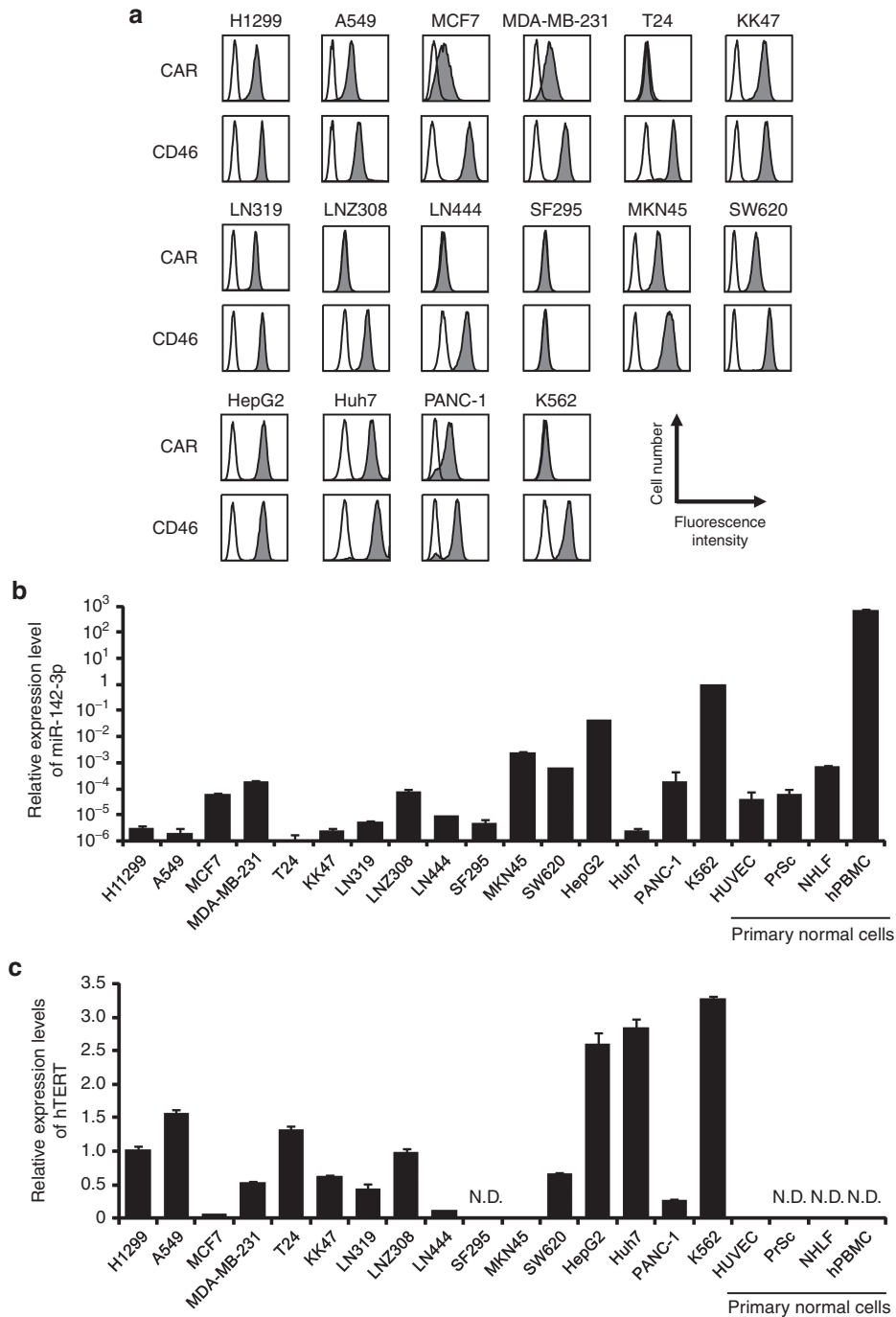


**Figure 2** Expression levels of coxsackievirus–adenovirus receptor (CAR), CD46, miR-142-3p, and human telomerase reverse transcriptase (hTERT) in the human cancer cell lines. **(a)** Surface expression levels of CAR and CD46 were assessed by flow cytometry. Open histograms represent isotype control staining. Filled histograms represent specific staining with anti-CAR antibody or anti-CD46 antibody. The data shown are representative of multiple measurements. **(b)** Expression levels of miR-142-3p were determined by real-time RT-PCR. The ratios of miR-142-3p to RNU6B levels were determined. The ratio of K562 cells was normalized to 1. **(c)** mRNA levels of hTERT were determined by real-time RT-PCR. The ratios of hTERT to GAPDH levels were determined. The ratio of H1299 cells was normalized to 1. Data are expressed as the mean  $\pm$  SD ( $n = 3$ ). ND, not detected.

tumor cell lines except for HepG2 cells (Figure 2b). All tumor cell lines examined, except for SF295 cells, exhibited detectable levels of hTERT mRNA expression, while hTERT expression was not detectable on primary normal cells, including PBMCs (Figure 2c). These results suggest that rAdF35-142T-GFP-mediated GFP expression would be disturbed by miR-142-3p in blood cells. With respect to the adherent tumor cell lines, HepG2 cells expressed more than 10-fold higher levels of miR-142-3p than the other adherent tumor cell lines.

rAdF35-142T-GFP-mediated GFP expression in cultured tumor cells  
Next, in order to examine whether rAdF35-142T-GFP efficiently mediates GFP expression in both CAR-positive and CAR-negative tumor

cells, more than 10 human tumor cell lines were transduced with the conditionally replicating Ads. rAd-GFP, rAdF35-GFP, and rAdF35-142T-GFP efficiently mediated GFP expression in most of the CAR-positive tumor cell lines (Figure 3a). More than 60% of the tumor cells were GFP positive at a multiplicity of infection (MOI) of 10. Time course profiles of the GFP expression were also comparable for these Ads in CAR-positive H1299 cells (Figure 3b). On the other hand, GFP expression was relatively low in MCF7, MDA-MB-231, and MKN45 cells following infection with rAd-GFP. In addition, CAR-negative tumor cells, including T24, LNZ308, and LN444 cells, were resistant to rAd-GFP. Less than 20% of the CAR-negative tumor cells were GFP positive. In contrast, rAdF35-GFP and rAdF35-142T-GFP produced more than 80% GFP-positive cells at an MOI of 10 in the CAR-negative tumor cells. rAdF35-142T-GFP also

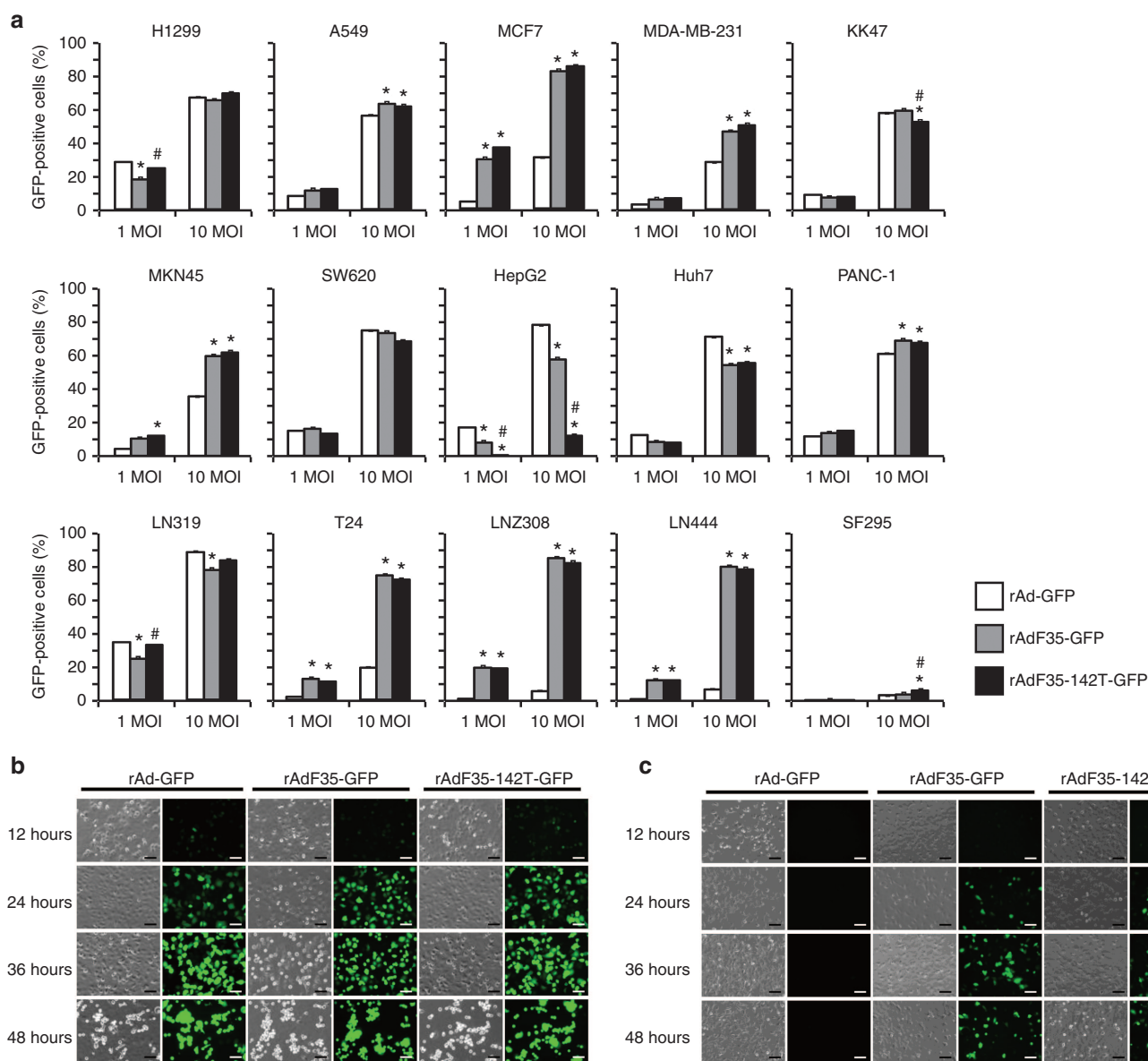


**Figure 3** Green fluorescence protein (GFP) expression levels in the tumor cell lines following infection with the conditionally replicating Ads. (a) The cell suspensions were incubated with the conditionally replicating Ads at MOIs of 1 and 10. Following a 24-hour incubation, the GFP expression levels were determined by flow cytometry. Data are expressed as the mean  $\pm$  SD ( $n = 3$ ). \* $P < 0.001$  in comparison with rAd-GFP. # $P < 0.001$  in comparison with rAdF35-GFP by one-way analysis of variance followed by Shapiro–Wilk’s analysis. Time-lapse images of (b) coxsackievirus–adenovirus receptor (CAR)-positive and (c) CAR-negative tumor cells following infection with the conditionally replicating Ads. (b) H1299 cells and (c) T24 cells were infected at an MOI of 10. Selected images taken at the indicated time points show cell morphology by phase-contrast microscopy (right panels) and GFP expression under fluorescence microscopy (left panels). Bar = 100  $\mu$ m.

efficiently mediated GFP expression in the other CAR-negative cell lines (Supplementary Figure S1A). Even in the CAR-positive tumor cells other than HepG2 cells, rAdF35-GFP and rAdF35-142T-GFP mediated almost comparable or higher levels of GFP expression, compared with rAd-GFP. HepG2 cells expressed lower levels of GFP following infection with rAdF35-142T-GFP than rAd-GFP and rAdF35-GFP, probably due to miR-142-3p expression. Comparison between the GFP expression levels in rAdF35-GFP-infected and rAdF35-142T-GFP-infected tumor cells indicated that insertion of the miR-142-3p-targeted sequences into the E1 and GFP expression cassettes did not disturb the GFP expression in tumor cells. Time course profiles of the GFP expression were also comparable for rAdF35-142T-GFP and rAdF35-GFP, although GFP-positive cells were almost undetectable for rAd-GFP in CAR-negative T24 cells (Figure 3c). Not only rAd-GFP but also rAdF35-142T-GFP mediated efficient GFP expression in EpCAM-negative tumor cell lines, which the CellSearch™ system would not detect (Supplementary Figure S1B). These results indicate that substitution with Ad35 fiber protein made it

possible to efficiently label CAR-positive and CAR-negative tumor cells with GFP.

rAdF35-142T-GFP-mediated GFP expression in tumor cells undergoing EMT and breast cancer stem cell-like CD24<sup>-/low</sup> CD44<sup>+</sup> cells

Next, in order to examine whether tumor cells undergoing EMT could be efficiently detected by rAdF35-142T-GFP, PANC-1 cells were cultured in the presence of transforming growth factor (TGF)-β for induction of EMT and were subsequently infected with the conditionally replicating Ads. EMT is often associated with CTCs.<sup>25-27</sup> Following a 6-day culture in the presence of TGF-β, the morphology of PANC-1 cells changed from a cobblestone-like epithelial phenotype to a spindle-like cell shape (Figure 4a). The expression levels of EMT marker genes, including *Snail* and *Slug*, were significantly upregulated by more than 100-fold (Figure 4b). On the other hand, the expressions of *E-cadherin* and *EpCAM* were significantly reduced.

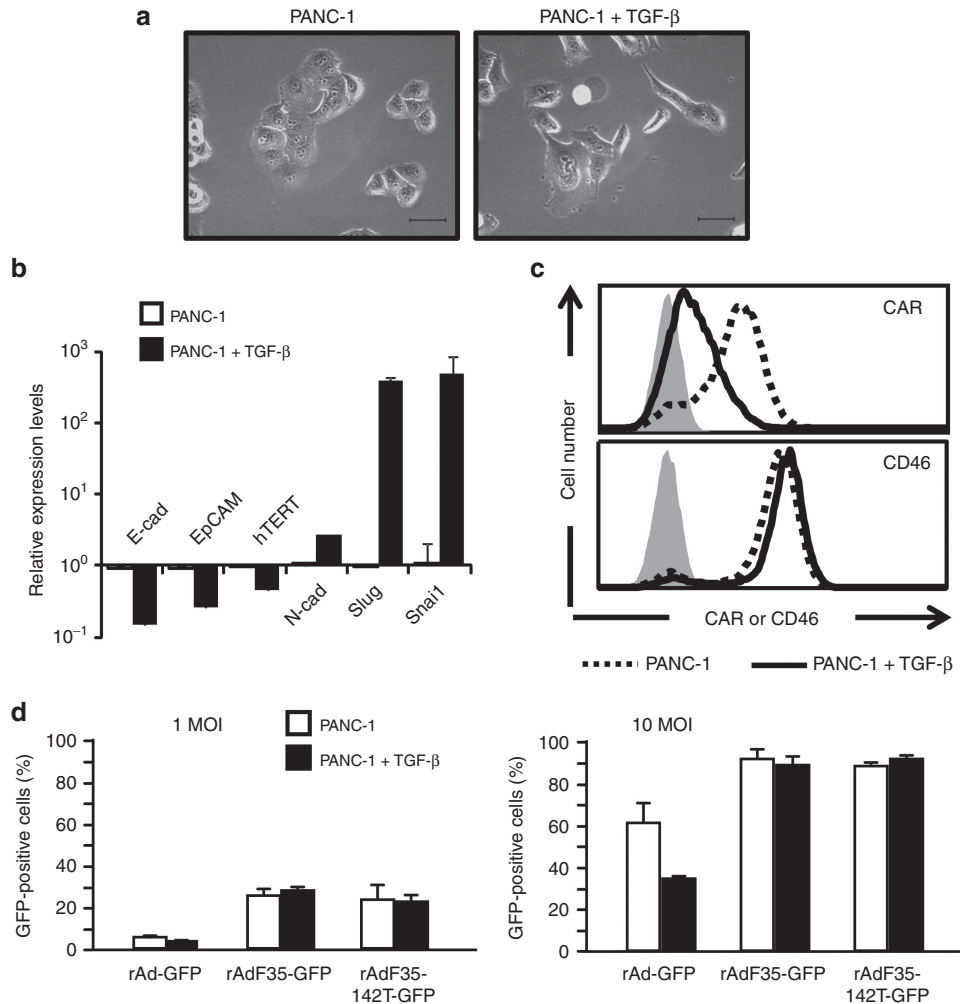


**Figure 4** Green fluorescence protein (GFP) expression following infection with the conditionally replicating Ads in the tumor cells undergoing TGF-β-induced epithelial-mesenchymal transition (EMT). (a) Cell morphology images of PANC-1 cells cultured in the presence of transforming growth factor (TGF)-β for 6 days were taken using a phase-contrast microscope. The images shown are representative of multiple experiments. Bar = 75 μm. (b) mRNA levels of EMT marker genes in PANC-1 cells undergoing EMT. The ratios of EMT marker genes to GAPDH were determined. The ratios in PANC-1 cells without TGF-β treatment were normalized to 1. Data are expressed as the mean ± SD (n = 3). (c) Surface expression levels of coxsackievirus-adenovirus receptor (CAR) and CD46 on PANC-1 cells undergoing EMT. The data shown are representative of multiple experiments. (d) GFP expression levels in PANC-1 cells undergoing EMT following infection with the conditionally replicating Ads. PANC-1 cells were infected with the conditionally replicating Ads at MOIs of 1 and 10. GFP expression levels were determined by flow cytometry 24 hours after infection. The data are expressed as the mean ± SD (n = 3).

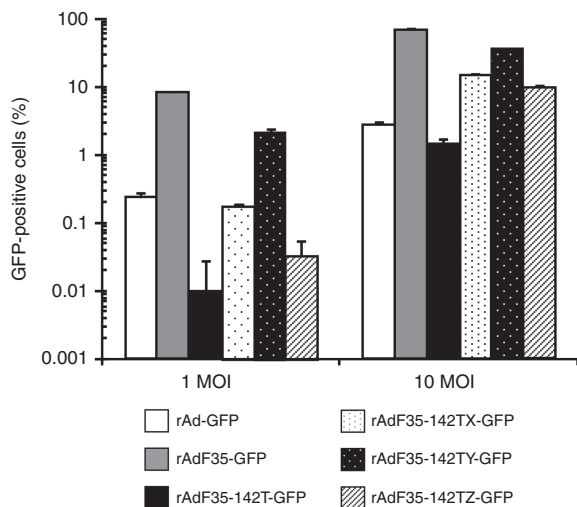


**Figure 5** Green fluorescence protein (GFP) expression levels in cells of the human myelogenous leukemia cell line K562 following infection with the conditionally replicating Ad derivatives containing different copy numbers of miR-142-3p–targeted sequences (see Supplementary Table S1). K562 cells were infected with the Ads at the indicated MOIs for 24 hours. GFP expression levels were determined by flow cytometry. Data are expressed as the mean  $\pm$  SD ( $n = 3$ ).

These results indicate that a 6-day culture in the presence of TGF- $\beta$  successfully induced EMT in PANC-1 cells. CAR expression was largely reduced on PANC-1 cells undergoing EMT (Figure 4c). The percentage of CAR-positive cells decreased from 80% to 24%, while no apparent changes in CD46 expression were found. rAdF35-142T-GFP and rAdF35-GFP efficiently mediated GFP expression (more than 90% GFP-positive cells at an MOI of 10) in both parental PANC-1 and PANC-1 cells undergoing EMT, although rAd-GFP-mediated GFP-positive cells were less than 40% in PANC-1 undergoing EMT, probably due to a decline in CAR expression (Figure 4d). These results indicate that CTCs which undergo EMT and exhibit a reduction in CAR expression are efficiently detected by rAdF35-142T-GFP and rAdF35-GFP, not rAd-GFP.

In order to examine whether cancer stem cell (CSC)–like cells could be detected by rAdF35-142T-GFP, CD24<sup>–low</sup> CD44<sup>+</sup> MCF7 cells were infected with the conditionally replicating Ads. Several studies have reported that CSC-like cells are often included in CTCs.<sup>28–30</sup> The CD24<sup>–low</sup> CD44<sup>+</sup> fraction was sorted from adriamycin (ADR)-resistant MCF7 (MCF7-ADR) cells, which is a human breast cancer cell line (Supplementary Figure S2A). CSC-like cells among breast cancer cells have been demonstrated to be rich in CD24<sup>–low</sup> CD44<sup>+</sup> fraction.<sup>31</sup> MCF7-ADR cells efficiently expressed both CAR and CD46 (Supplementary Figure S2B). When CD24<sup>–low</sup> CD44<sup>+</sup> MCF7-ADR cells were infected with the Ads, more than 70% GFP-positive cells were obtained by rAd-GFP, rAdF35-142T-GFP, and rAdF35-GFP at an MOI of 10; however, slightly but significantly higher percentages of GFP-positive cells were found by rAdF35-142T-GFP and rAdF35-GFP than by rAd-GFP at an MOI of 10 (Supplementary Figure S2C). These results indicate that rAdF35-142T-GFP and rAdF35-GFP efficiently mediate GFP expression in CSC-like cells, leading to efficient detection of CSC-like cells in CTCs.

Significant reduction in false-positive PBMCs by incorporation of miR-142-3p–targeted sequences

In order to examine whether incorporation of miR-142-3p–targeted sequences into the 3′-UTR of the E1B and GFP genes results in

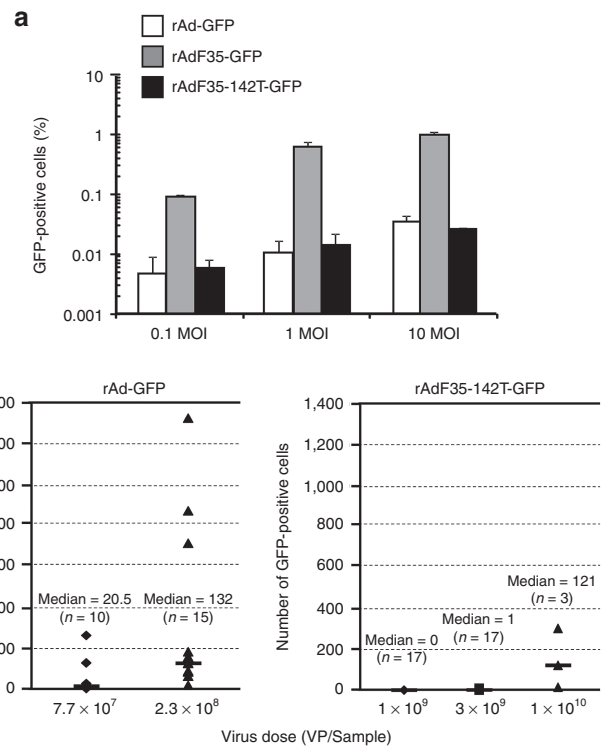


**Figure 6** Green fluorescence protein (GFP) expression in peripheral blood mononuclear cells (PBMCs) from healthy donors following infection with the conditionally replicating Ads. **(a)** Flow cytometric analysis of GFP expression in PBMCs following infection with the conditionally replicating Ads. PBMCs were infected with the Ads at MOIs of 0.1, 1, and 10 for 24 hours. Data are expressed as the mean  $\pm$  SD ( $n = 3$ ). **(b)** Detection of GFP-positive PBMCs by fluorescence microscopy following infection with the Ads. PBMCs from healthy donors were infected with the indicated amounts of Ads for 24 hours. Numbers of GFP-positive cells were counted by fluorescence microscopy.

reduction in false (GFP)-positive PBMCs following infection, GFP expression in the blood cells was determined following infection. First, in order to examine the effects of copy numbers of miR-142-3p–targeted sequences in the 3′-UTR of the E1B and GFP genes on the suppression levels of GFP expression in blood cells, cells of a human myelogenous leukemia cell line, K562, were infected with rAdF35-142T-GFP derivatives containing the various copy numbers of miR-142-3p–targeted sequences (Supplementary Table S1). Flow cytometric analysis demonstrated that rAdF35-142T-GFP, which contains four copies of miR-142-3p–targeted sequences in the 3′-UTR of both the E1B and GFP genes, exhibited lower GFP expression in K562 cells than the other types of Ads (Figure 5), indicating that four copies of miR-142-3p–targeted sequences in the 3′-UTR of both the E1B and GFP genes are necessary to efficiently suppress the GFP expression in the blood cells.

Next, PBMCs were infected with the conditionally replicating Ads. rAd-GFP mediated 0.011% and 0.034% GFP-positive cells at MOIs of 1 and 10, respectively (Figure 6a). On the other hand, infection with rAdF35-GFP resulted in 0.62% and 0.98% GFP-positive cells at MOIs of 1 and 10, respectively; however, GFP-positive PBMCs were dramatically reduced for rAdF35-142T-GFP. Infection with rAdF35-142T-GFP at MOIs of 1 and 10 resulted in 0.014% and 0.027% GFP-positive cells, respectively. These results indicate that substitution with Ad35 fiber protein increases GFP-positive PBMCs; however, incorporation of miR-142-3p–targeted sequences into the 3′-UTR of the E1B and GFP genes largely suppresses GFP expression in PBMCs.

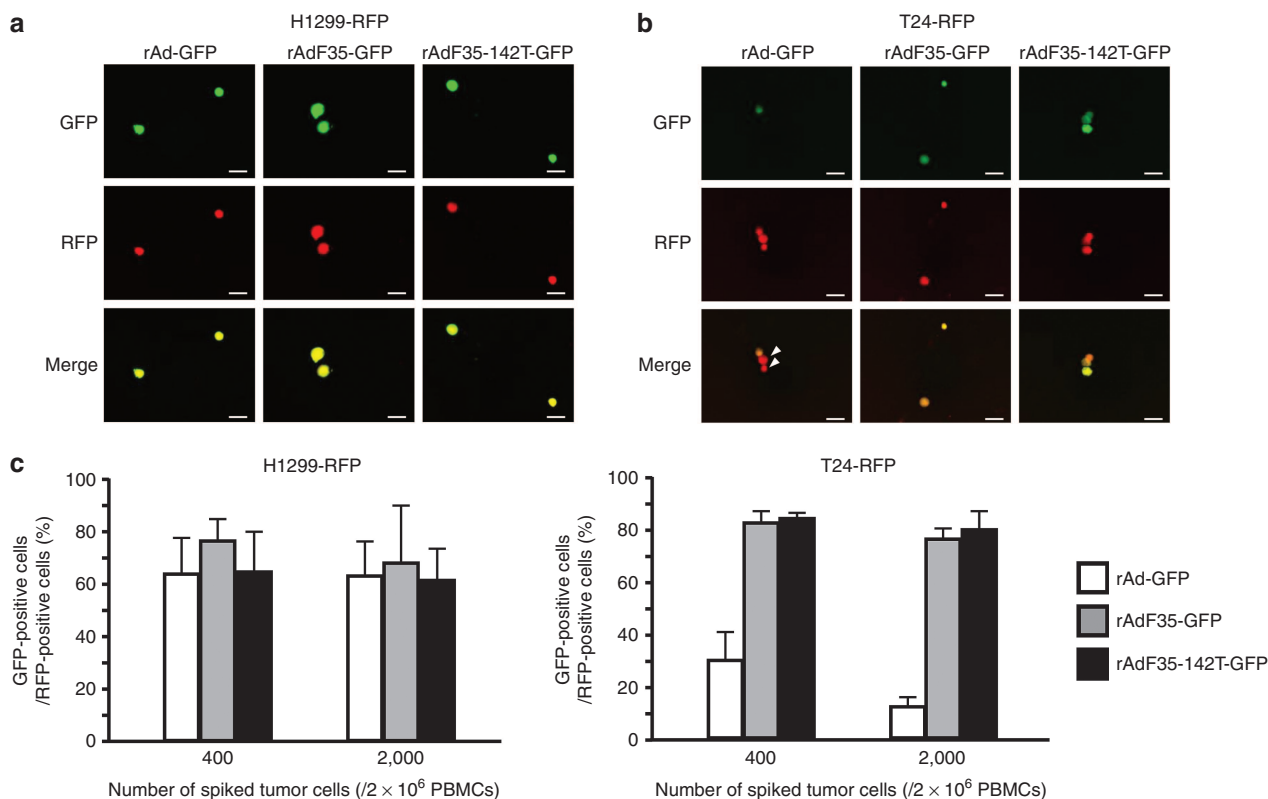


**Figure 7** Detection of human cancer cells spiked into peripheral blood mononuclear cells (PBMCs) by the conditionally replicating Ads. H1299 and T24 cells stably expressing red fluorescent protein (RFP) were spiked into PBMCs. The cells were then infected with the Ads for 24 hours. Fluorescence images of (a) H1299 and (b) T24 cells following infection with the Ads. RFP-expressing H1299 and T24 cells ( $1 \times 10^5$  cells) were spiked into  $5 \times 10^6$  PBMCs. The cells suspended in 1 ml of RPMI1640 medium were incubated with  $2 \times 10^7$  IFU of the Ads for 24 hours. The expression of green fluorescence protein (GFP) and RFP was observed under a fluorescence microscope. White arrowheads indicate uninfected tumor cells. The images shown are representative of multiple experiments. Bar = 50  $\mu$ m. (c) Efficiencies of GFP labeling of human cancer cells spiked into PBMCs. RFP-expressing H1299 and T24 cells were spiked into  $2 \times 10^6$  PBMCs. The cells suspended in 1 ml of RPMI1640 medium were infected with  $2 \times 10^7$  IFU of the Ads for 24 hours. Measurement of GFP and RFP expression in the cells was carried out by flow cytometry. Data are shown as the mean  $\pm$  SD ( $n = 3$ ).

In the experiments described above, incorporation of miR-142-3p-targeted sequences into the 3'-UTR of the E1B and GFP genes largely reduced GFP-positive PBMCs; however, detectable levels of GFP expression were still found by flow cytometry following infection with rAdF35-142T-GFP, because flow cytometry can sensitively detect a much low level of GFP expression (Supplementary Figure S3). In order to examine whether GFP-positive PBMCs could still be detected following infection with rAdF35-142T-GFP by the fluorescence microscopy system used for GFP-positive CTC detection in the previous study,<sup>10</sup> GFP expression was observed under a fluorescence microscope. When PBMCs recovered from the 7.5 ml blood samples of healthy volunteers (approximately  $1-2 \times 10^7$  cells) were incubated with  $1 \times 10^6$  IFU and  $3 \times 10^6$  IFU of rAd-GFP, 20.5 and 132 GFP-positive PBMCs were found on average (Figure 6b). On the other hand, no or much low numbers of GFP-positive PBMCs was detected by rAdF35-142T-GFP. These results indicate that false-positive PBMCs can be significantly reduced by rAdF35-142T-GFP, making it possible to accurately detect CTCs without producing false-positive cells.

#### Detection of tumor cells spiked into PBMCs

In order to examine whether CAR-positive and CAR-negative tumor cells in the blood were efficiently labeled with GFP by rAdF35-142T-GFP, CAR-positive H1299 cells and CAR-negative T24 cells expressing red fluorescent protein (RFP) were spiked into PBMCs

and incubated with either rAd-GFP or rAdF35-142T-GFP. More than 80% of the spiked tumor cells (RFP-positive cells) were recovered for assessment of GFP expression. H1299 cells were efficiently labeled with GFP by all types of conditionally replicating Ads (Figure 7a,c). More than 60% of GFP-positive H1299 cells were labeled with GFP. On the other hand, less than 30% of CAR-negative T24 cells were labeled with GFP by rAd-GFP (Figure 7b,c); however, incubation with rAdF35-GFP and rAdF35-142T-GFP efficiently mediated more than 75% GFP-positive T24 cells. More than 70% of CAR-positive A549 cells were labeled with GFP by both rAd-GFP and rAdF35-142T-GFP when 100 A549 cells were spiked into 7.5 ml blood of healthy volunteers (Supplementary Figure S4). These results indicate that rAdF35-142T-GFP efficiently detects both CAR-positive and CAR-negative CTCs, while rAd-GFP detected only CAR-positive CTCs.

#### Detection of CTCs in the blood isolated from cancer patients

Next, in order to examine the CTC detection profiles in the blood isolated from cancer patients by the conditionally replicating Ads, rAd-GFP and rAdF35-142T-GFP were added to the blood isolated from non-small-cell lung cancer (NSCLC) patients, followed by immunostaining with anti-CD45 antibody. Immunostaining with anti-CD45 antibody is an effective method to distinguish GFP signals between tumor cells and blood cells.<sup>11</sup> Previous studies reported that CTCs are a promising biomarker even in NSCLC patients.<sup>32,33</sup> In this experiment,  $2.3 \times 10^8$  virus particles (VP) of rAd-GFP was added to the

samples because higher titers of rAd-GFP were expected to produce large numbers of false-positive cells. On the other hand,  $1 \times 10^9$  VP of rAdF35-142T-GFP was used due to the low levels of production of false-positive cells, as shown in Figure 5. In addition, we considered that high titers of rAdF35-142T-GFP were necessary to efficiently mediate GFP expression in CTCs, because we considered that efficient binding of rAdF35-142T-GFP to PBMCs via CD46 might prevent rAdF35-142T-GFP from infecting CTCs. CTCs and false-positive cells were defined as GFP<sup>+</sup>/CD45<sup>-</sup> and GFP<sup>+</sup>/CD45<sup>+</sup> cells, respectively.

We successfully detected CTCs in the blood samples isolated from NSCLC patients by both rAdF35-142T-GFP and rAd-GFP (Table 1). Following treatment with rAd-GFP, 2.3 CTCs per sample were detected on average in 11 of 15 samples (73.3% of the samples tested). The number of CTCs detected in 7.5 ml samples by rAd-GFP ranged from 0 to 8; however, more than 70 false-positive cells (528 false-positive cells per sample on average, with a range from 73 to 2902 cells) were produced per sample by rAd-GFP. The percentage of false-positive cells (false-positive rate) was 99.0%. On the other hand, 17 of 40 samples were CTC positive following treatment with rAdF35-142T-GFP (42.5% of the samples tested) (0.9 CTCs per sample on average, with a range from 0 to 7 CTCs). The percentages of false-positive cells were 49.7% (1.8 false-positive cells per sample on average, with a range from 0 to 12 cells) for rAdF35-142T-GFP. When rAd-GFP or rAdF35-142T-GFP was added to blood samples isolated from the same patients (J-317, J-318, J-335, J-337~J-340), rAdF35-142T-GFP detected no CTCs in these patients, although rAd-GFP detected CTCs in four of seven patients. Among the CTC-positive samples, the percentages of CTC/total GFP-expressing cells, which are considered to represent the true-positive rate, by rAd-GFP and rAdF35-142T-GFP were 1.4% and 71.1%, respectively (Supplementary Figure S5). These results indicate that while most of the rAd-GFP-mediated GFP-positive cells were false-positive cells, rAdF35-142T-GFP exhibited more accurate detection of CTCs than rAd-GFP under these experimental conditions. These data suggest that a rAdF35-142T-GFP-based assay system can more efficiently and accurately detect CTCs than a rAd-GFP-based assay system.

## DISCUSSION

The aim of this study was to develop an efficient CTC detection system that exhibits both suppression of the production of false-positive cells and detection of both CAR-positive and CAR-negative CTCs by using a novel conditionally replicating Ad. For this purpose, target sequences of miR-142-3p were incorporated into the 3'-UTR of the E1B and GFP genes to inhibit the expression of these genes in blood cells. In addition, the Ad fiber proteins were replaced with fiber proteins of Ad35 in order to infect CTCs via binding to CD46 as a receptor.

In this study, blood cells were incubated with larger amounts of the conditionally replicating Ads than were used in the previous study. Kojima *et al.* reported that  $1 \times 10^4$  plaque forming unit of rAd-GFP were incubated with blood cells isolated from 5 ml of blood,<sup>10</sup> while in the present study the blood cells recovered from 7.5 ml of blood (approximately  $1-2 \times 10^7$  cells) were infected with  $1 \times 10^9$  VP of rAdF35-142T-GFP (Table 1). We considered that the amounts of rAdF35-142T-GFP required to efficiently infect CTCs would be larger than the amounts of rAd-GFP required to achieve the same goal since efficient binding of rAdF35-142T-GFP to not only CTCs but also PBMCs would occur due to CD46 expression on both CTCs and PBMCs, leading to sequestration of rAdF35-142T-GFP by PBMCs. However, the data in Figure 7 indicate that the sequestration of rAdF35-142T-GFP by PBMCs would have only minimal influence on the GFP expression levels on CTCs. Even at

high titers of rAdF35-142T-GFP, few false-positive cells were found in this study, permitting accurate counting of CTCs. Increases in the titers of rAdF35-142T-GFP added to the samples also led to efficient labeling of CTCs with GFP. On the other hand, high titers of rAd-GFP cannot be used because large numbers of false-positive cells were produced by high titers of rAd-GFP. More than 70 false-positive cells were found even at  $3 \times 10^6$  IFU of rAd-GFP, although the levels of false-positive cells produced by  $1 \times 10^8$  IFU of rAdF35-142T-GFP in these patients were almost negligible (Table 1). Blood cells in cancer patients might be more susceptible to Ads than those in healthy donors. The median number of GFP-positive blood cells was 132 following infection with rAd-GFP in the transduction experiment using PBMCs from healthy donors (Figure 5b), while the median number of GFP-positive blood cells (false-positive cells) in the cancer patients was 401 following rAd-GFP infection (Table 1). Previous studies demonstrated that a conventional Ad vector transduced blood cells via the interaction between  $\alpha_v$ -integrins on the cell surface and the RGD (arginine-glycine-aspartic acid) motif in the penton base due to the lack of CAR expression on blood cells.<sup>34,35</sup> Granulocyte macrophage-colony stimulating factor (GM-CSF) and macrophage-colony stimulating factor (M-CSF) elevated the  $\alpha_v$ -integrin expression on blood cells, leading to upregulation in Ad vector-mediated transduction.<sup>34</sup> In other studies, blood concentrations of GM-CSF and M-CSF were reported to be elevated in cancer patients compared with those in healthy donors.<sup>36,37</sup> GFP-positive normal blood cells were distinguished from CTCs via immunostaining with anti-human CD45 antibody. Staining with anti-CD45 antibody was highly efficient; however, not all of the CD45<sup>+</sup> cells would have been detected by the treatment with anti-CD45 antibody. It might be possible that GFP<sup>+</sup>/CD45<sup>-</sup> cells, which were defined as CTCs in this study, contained normal blood cells due to a failure of immunostaining with anti-CD45 antibody. Therefore, GFP expression in normal blood cells should be suppressed as much as possible to reduce the numbers of false-positive cells. miR-142-3p-mediated suppression of GFP expression in normal blood cells is a highly promising strategy for such reduction of false-positive cells.<sup>38,39</sup>

Human CD46 was utilized as an infection receptor of a conditionally replicating Ad by replacing with Ad35 fiber protein in order to mediate GFP expression in CAR-negative CTCs in this study. Several strategies of recombinant Ad modifications have been adopted to confer GFP expression in CAR-negative cells. For example, fiber-substituting recombinant Ads containing fiber protein derived from Ad serotypes 3, 7, 11, and 14 can infect cells via desmoglein-2<sup>40</sup>; however, expression of desmoglein-2 is also downregulated under EMT.<sup>41</sup> Genetic incorporation of poly-lysines and Arg-Gly-Asp (RGD) peptides into the fiber knob makes it possible for a recombinant Ad to infect *via* heparan sulfate and  $\alpha_v$ -integrins, respectively<sup>42-44</sup>; however, downregulation of heparin sulfate was reported in several types of tumors.<sup>45,46</sup> Although fiber-modified conditionally replicating Ads containing RGD peptides in the fiber knob infect CTCs via interaction with  $\alpha_v$ -integrins, CD46 is an infection receptor suitable for infection of CTCs with conditionally replicating Ads because CD46 was upregulated in malignant tumor cells.<sup>19,20</sup> In addition, CD46 was not downregulated under TGF- $\beta$ -induced EMT (Figure 4). It has not been reported whether CAR expression on CTCs is downregulated. A previous study demonstrated that detectable levels of CAR were found in CTCs by microarray analysis, although CTCs were recovered by the CellSearch system, which is difficult to detect EpCAM-negative CTCs<sup>47</sup>; however, CAR expression is often reduced in malignant tumor cells, including tumor cells undergoing EMT.<sup>15,16</sup> A conditionally replicating Ad should infect CTCs via a receptor

**Table 1.** Detection of CTCs in the patients with non-small-cell lung cancer

Case number of cancer patients	Cell number			Rate	
	Total GFP <sup>+</sup> cells	CTCs	False-positive cells	True-positive cells (%)	False-positive cells (%)
<b>rAd-GFP (n = 15)</b>					
J-101	86	0	86	0.00	100.00
J-102	73	3	70	4.10	95.90
J-104	181	5	176	2.80	97.20
J-105	644	1	643	0.20	99.80
J-106	89	2	87	2.20	97.80
J-107	275	8	267	2.90	97.10
J-109	489	2	487	0.40	99.60
J-110	154	1	153	0.60	99.40
J-317	500	0	500	0.00	100.00
J-318	2,902	3	2,899	0.10	99.90
J-335	892	4	888	0.40	99.60
J-337	423	0	423	0.00	100.00
J-338	403	2	401	0.50	99.50
J-339	440	0	440	0.00	100.00
J-340	403	3	400	0.70	99.30
<b>Total</b>	7,954	34	7,920	—	—
<b>Average</b>	530.3	2.3	528	1.00	99.00
<b>SD</b>	694.5	2.2	694.4	1.30	1.30
<b>Median</b>	403	2	401	—	—
<b>rAdF35-142T-GFP (n = 40)</b>					
J-201	7	2	5	28.60	71.40
J-203	4	2	2	50.00	50.00
J-204	0	0	0	—	—
J-205	1	1	0	100.00	0.00
J-206	2	2	0	100.00	0.00
J-207	1	1	0	100.00	0.00
J-208	0	0	0	—	—
J-210	2	0	2	0.00	100.00
J-211	11	0	11	0.00	100.00
J-212	8	2	6	25.00	75.00
J-213	7	1	6	14.30	85.70
J-214	13	1	12	7.70	92.30
J-216	0	0	0	—	—
J-217	2	2	0	100.00	0.00
J-218	0	0	0	—	—
J-221	4	0	4	0.00	100.00
J-222	0	0	0	—	—
J-223	1	0	1	0.00	100.00
J-301	1	1	0	100.00	0.00

**Table 1.** Continued

Case number of cancer patients	Cell number			Rate	
	Total GFP <sup>+</sup> cells	CTCs	False-positive cells	True-positive cells (%)	False-positive cells (%)
J-302	2	1	1	50.00	50.00
J-303	1	1	0	100.00	0.00
J-304	1	1	0	100.00	0.00
J-305	1	0	1	0.00	100.00
J-306	0	0	0	—	—
J-307	0	0	0	—	—
J-308	1	0	1	0.00	100.00
J-309	7	5	2	71.40	28.60
J-310	1	0	1	0.00	100.00
J-312	9	7	2	77.80	22.20
J-313	0	0	0	—	—
J-317	0	0	0	—	—
J-318	0	0	0	—	—
J-334	0	0	0	—	—
J-335	0	0	0	—	—
J-336	6	5	1	83.30	16.70
J-337	4	0	4	0.00	100.00
J-338	7	0	7	0.00	100.00
J-339	1	0	1	0.00	100.00
J-340	2	0	2	0.00	100.00
J-341	1	1	0	100.00	0.00
<b>Total</b>	108	36	72	—	—
<b>Average</b>	2.7	0.9	1.8	43.10	56.9
<b>SD</b>	3.4	1.6	3	44.20	49.2
<b>Median</b>	1	0	0.5	—	—

CTC, GFP<sup>+</sup>CD45<sup>-</sup> cells; false-positive cells, GFP<sup>+</sup>CD45<sup>+</sup> cells.  
True-positive rate, CTC/total GFP<sup>+</sup> cells; false-positive rate, false-positive cells/total GFP<sup>+</sup> cells.  
CTC, circulating tumor cell; GFP, green fluorescence protein.

different from CAR in order to efficiently detect both CAR-positive and CAR-negative CTCs.

miR-142-3p was utilized to suppress the expression of the E1 and GFP genes in blood cells in this study. Previous studies demonstrated that miR-142-3p is highly and specifically expressed in various types of blood cells, including T cells, B cells, and granulocytes<sup>13,48</sup> and that incorporation of miR-142-3p-targeted sequences into the 3'-UTR of the transgene efficiently and specifically suppressed the transgene expression in blood cells.<sup>49,50</sup> On the other hand, CTCs of breast cancer patients expressed much lower levels of miR-142-3p than normal leukocytes.<sup>14</sup> The data in both this study and previous studies suggest that miR-142-3p is the most suitable for suppression of transgene expression via an miRNA-regulated transgene expression system in blood cells; however, miR-142-3p expression is relatively low in several types of blood cells. For example, regulatory T cells

expressed lower levels of miR-142-3p than conventional T cells.<sup>51</sup> miR-142-3p expression in CD4<sup>+</sup> T cells of systemic lupus erythematosus patients was lower than that in the CD4<sup>+</sup> T cells of healthy controls.<sup>52</sup> On the other hand, miR-142-3p expression was upregulated by triptolide and quercetin in pancreatic ductal adenocarcinoma cells.<sup>53</sup> We should pay attention to miR-142-3p expression levels in normal blood cells as well as tumor cells to correctly detect CTCs.

rAdF35-142T-GFP efficiently labeled both CAR-positive and CAR-negative tumor cells spiked into PBMCs (Figure 7); however, when rAd-GFP and rAdF35-GFP were added to blood samples from the same patients, CTCs were not detected by rAdF35-142T-GFP in these samples, in spite of the rAd-GFP-mediated production of GFP-positive CTCs in four of the seven patients (Table 1). It is unclear why rAdF35-142T-GFP failed to mediate GFP expression in the CTCs of these patients. As described above, some of the GFP-expressing blood cells might not have been stained with the anti-CD45 antibody. Alternatively, it is unlikely but nonetheless possible that a subpopulation of CTCs is more permissive to rAd-GFP than rAdF35-142T-GFP.

In summary, we developed a novel conditionally replicating Ad expressing GFP, rAdF35-142T-GFP, for efficient detection of CTCs without significant production of false-positive cells. The CTC detection method using rAdF35-142T-GFP would contribute to the progression of CTC-based diagnosis as well as the characterization of CTCs.

## MATERIALS AND METHODS

### Cell culture

Various types of human cultured tumor cell lines (Supplementary Table S2) and primary cells were cultured in a humidified atmosphere of 5% CO<sub>2</sub> at 37 °C according to the specifications supplied by the vendor. HepG2 cells and Huh7 cells were obtained from the JCRB Cell Bank (Tokyo, Japan). Human glioma cell lines, SF295, LN444, LN319, and LN2308 cells were kindly provided from Dr. M. Tada (Hokkaido University, Hokkaido, Japan). The other cell lines were obtained from ATCC. Cell master stocks were prepared, and cells for experiments were passaged for less than 6 months.

### Conditionally replicating Ads

rAd-GFP, which is a telomerase-specific replication-competent Ad possessing an hTERT promoter-driven E1 gene expression cassette in the E1-deleted region and a cytomegalovirus (CMV) promoter-driven GFP expression cassette in the E3-deleted region, and which is identical to OBP-401, was prepared as previously described.<sup>12</sup> A fiber-substituted rAd-GFP, named rAdF35-GFP, was produced by substituting the fiber protein of rAd-GFP with that of Ad35. An Ad plasmid for rAdF35-GFP was constructed by using pAdHM49,<sup>21</sup> pSh-hAIB,<sup>54</sup> and pHM11-EGFP-N2.<sup>12</sup> rAdF35-142T-GFP, which is a derivative of rAdF35-GFP possessing four copies of a sequence perfectly complementary to miR-142-3p in the 3'-UTR of the E1 gene and the GFP gene, was prepared as described below. Briefly, oligonucleotides encoding miR-142-3p complementary sequences (Supplementary Table S3) were cloned into pHMCMV5,<sup>55</sup> resulting in pHMCMV5-142-3pT. A fragment containing an hTERT promoter-driven E1 gene expression cassette was inserted into the upstream region of miR-142-3p complementary sequences in pHMCMV5-142-3pT, creating pHM5-hAIB-142-3pT. For construction of a GFP expression cassette containing miR-142-3p complementary sequences, oligonucleotides encoding miR-142-3p complementary sequences were inserted into the 3'-UTR of the GFP gene in pHMCMV-GFP1,<sup>56</sup> resulting in pHMCMV-GFP1-142-3pT. A GFP expression cassette containing miR-142-3p complementary sequences was recovered from pHMCMV-GFP1-142-3pT and cloned into pHM13,<sup>57</sup> creating pHM13-GFP-142-3pT. The E1 gene expression cassette was cloned into the E1-deleted region of pAdHM49, resulting in pAdHM49-hAIB-142-3pT. The GFP expression cassette was recovered from pHM13-GFP-142-3pT and inserted into the E3-deleted region of pAdHM49-hAIB-142-3pT, resulting in pAdHM49-hAIB-GFP-142-3pT. Further information on the plasmid construction is available on request. Recombinant Ads were produced by transfection of the *PacI*-digested Ad plasmids into H1299 cells.

All Ads were propagated in H1299 cells, purified by two rounds of cesium chloride-gradient ultracentrifugation, dialyzed, and stored at -80 °C. The VP titers were determined using a spectrophotometric method, and biological titers were measured using an Adeno-X-rapid titer kit (Clontech, Mountain View, CA).

### Expression analysis of CAR, CD46, hTERT, and miR-142-3p

Expression levels of human CAR and CD46 on the cell surface were measured by flow cytometry as previously described.<sup>58</sup> Copy numbers of miR-142-3p and hTERT mRNA were determined by real-time RT-PCR as previously described.<sup>12,50</sup>

### Analysis of GFP expression in human tumor cell lines

Human tumor cells were recovered from the culture dish and re-suspended to prepare tumor cell suspensions of 5 × 10<sup>4</sup> cells/ml. Five hundred microliters of each cell suspension was mixed with 50 μl of 5 × 10<sup>5</sup> and 5 × 10<sup>6</sup> infectious units (IFU)/ml of Ad suspensions in one well of a 24-well plate. Following a 24-hour incubation, the tumor cells were recovered, washed, and subjected to flow cytometric analysis for measurement of GFP expression.

### Induction of EMT

PANC-1 cells (a human pancreatic cancer cell line) were cultured in the presence of 10 ng/ml of TGF-β (PeproTech, Rocky Hill, NJ) for induction of EMT. Following a 6-day culture, the mRNA levels of EMT marker genes were evaluated by real-time RT-PCR. Primers for the EMT marker genes are shown in Supplementary Table S4. CAR and CD46 expression levels on the cells undergoing EMT were examined by flow cytometry.

### Analysis of GFP expression in normal blood cells

Generation of GFP-positive normal blood cells (false-positive cells) by the Ads was evaluated as follows; briefly, blood samples isolated from healthy volunteers were incubated with red blood cell lysis buffer to remove erythrocytes. Following washing and centrifugation, 1 × 10<sup>6</sup> cells of peripheral blood mononuclear cells (PBMCs) were incubated with the conditionally replicating Ads at the indicated MOIs in a 1 ml mixture at 37 °C. Following a 24-hour incubation, the percentage of GFP-positive cells was measured using flow cytometry. For the evaluation of false-positive cells by fluorescence microscopy, PBMCs recovered from the 7.5 ml blood samples of healthy volunteers were incubated with rAd-GFP and rAdF35-142T-GFP. Following a 24-hour incubation, the numbers of GFP-positive cells were counted under a fluorescence microscope as previously described.<sup>10</sup> PBMCs obtained from LONZA (Basel, Switzerland) were also used in this experiment. The study protocols described above were approved by the ethics committee of Osaka University and Kenshokai Fukushima Healthcare Center, which is the affiliated institution of Oncolys Biopharma. All volunteers provided written informed consent.

### Detection of tumor cells spiked into human PBMCs

Variable numbers of H1299 and T24 cells stably expressing RFP were spiked into 2 × 10<sup>6</sup> or 5 × 10<sup>6</sup> cells of PBMCs. The cell suspensions were mixed with 2 × 10<sup>7</sup> IFU of the Ads and were incubated at room temperature for 24 hours. GFP and RFP expression in the cells was analyzed by flow cytometry or fluorescence microscopy.

### Detection of CTCs in the blood samples of cancer patients

CTCs in the peripheral blood samples of cancer patients were detected as previously described with slight modifications.<sup>10</sup> Briefly, cells recovered from the 7.5 ml blood samples of patients with NSCLC were incubated with 2.3 × 10<sup>8</sup> VP of rAd-GFP and 1 × 10<sup>9</sup> VP of rAdF35-142T-GFP at 37 °C. Following a 24-hour incubation, the cells were washed and stained with anti-human CD45 antibody (clone HI30; Biolegend, San Diego, CA), then observed by fluorescence microscopy. CTCs and false-positive cells were defined as GFP<sup>+</sup>/CD45<sup>-</sup> and GFP<sup>+</sup>/CD45<sup>+</sup> cells, respectively. The procedures for obtaining peripheral blood from patients with lung cancer were approved by the Institutional Review Board at the Juntendo University School of Medicine (No. 2013067). All patients provided written informed consent.

## Statistical analysis

Data are shown as means  $\pm$  SD. For comparisons between two groups, significant differences were determined by the one-way analysis of variance followed by Shapiro–Wilk's analysis. In the experiments using blood samples of cancer patients, the numbers of GFP-positive cells were compared between groups using the Mann–Whitney U test. Comparisons were considered statistically significant at  $P < 0.05$ . All statistical analyses were performed with GraphPad prism software for Macintosh (GraphPad Software, La Jolla, CA).

## CONFLICT OF INTEREST

T.F. and H.M. are consultants of Oncolys BioPharm. Y.U. is President and CEO of Oncolys BioPharm. M.O. and N.K. are employees of Oncolys Biopharma. F.S. and H.M. have the potential to receive patent royalties from Oncolys BioPharm. No potential conflicts of interest were disclosed by the other authors.

## ACKNOWLEDGMENTS

This work was supported in part by a Grant-in-Aid for Young Scientists (A) to F.S. and Scientific Research (A) to H.M. from the Ministry of Education, Culture, Sports, Sciences, and Technology (MEXT) of Japan and grants from Hyogo Science and Technology Association to F.S., the Japan Research Foundation for Clinical Pharmacology to F.S., Mochida Memorial Foundation for Medical and Pharmaceutical Research to H.M., YOKOYAMA foundation for Clinical Pharmacology to M.T., and Daiwa Securities Health Foundation to F.S. K.T. and M.M. are Research Fellows of the Japan Society for the Promotion of Science. The authors thank Sayuri Okamoto (Osaka University, Osaka, Japan) for her help. The authors also thank Takahiro Ochiya (National Cancer Center Research Institute, Tokyo, Japan) for providing MCF7-ADR cells.

## REFERENCES

- Cristofanilli, M, Budd, GT, Ellis, MJ, Stopeck, A, Matera, J, Miller, MC *et al.* (2004). Circulating tumor cells, disease progression, and survival in metastatic breast cancer. *N Engl J Med* **351**: 781–791.
- Danila, DC, Fleisher, M and Scher, HI (2011). Circulating tumor cells as biomarkers in prostate cancer. *Clin Cancer Res* **17**: 3903–3912.
- Lianidou, ES, Mavroudis, D and Georgoulas, V (2013). Clinical challenges in the molecular characterization of circulating tumour cells in breast cancer. *Br J Cancer* **108**: 2426–2432.
- Kang, Y and Pantel, K (2013). Tumor cell dissemination: emerging biological insights from animal models and cancer patients. *Cancer Cell* **23**: 573–581.
- Nagrath, S, Sequist, LV, Maheswaran, S, Bell, DW, Irimia, D, Ulkus, L *et al.* (2007). Isolation of rare circulating tumour cells in cancer patients by microchip technology. *Nature* **450**: 1235–1239.
- Androulakis, N, Agelaki, S, Perraki, M, Apostolaki, S, Bozionelou, V, Pallis, A *et al.* (2012). Clinical relevance of circulating CK-19mRNA-positive tumour cells before front-line treatment in patients with metastatic breast cancer. *Br J Cancer* **106**: 1917–1925.
- Königsberg, R, Obermayr, E, Bises, G, Pfeiler, G, Gneist, M, Wrba, F *et al.* (2011). Detection of EpCAM positive and negative circulating tumor cells in metastatic breast cancer patients. *Acta Oncol* **50**: 700–710.
- Rao, CG, Chianese, D, Doyle, GV, Miller, MC, Russell, T, Sanders, RA Jr. *et al.* (2005). Expression of epithelial cell adhesion molecule in carcinoma cells present in blood and primary and metastatic tumors. *Int J Oncol* **27**: 49–57.
- Zhang, L, Ridgway, LD, Wetzel, MD, Ngo, J, Yin, W, Kumar, D *et al.* (2013). The identification and characterization of breast cancer CTCs competent for brain metastasis. *Sci Transl Med* **5**: 180ra48.
- Kojima, T, Hashimoto, Y, Watanabe, Y, Kagawa, S, Uno, F, Kuroda, S *et al.* (2009). A simple biological imaging system for detecting viable human circulating tumor cells. *J Clin Invest* **119**: 3172–3181.
- Takakura, M, Kyo, S, Nakamura, M, Maida, Y, Mizumoto, Y, Bono, Y *et al.* (2012). Circulating tumour cells detected by a novel adenovirus-mediated system may be a potent therapeutic marker in gynaecological cancers. *Br J Cancer* **107**: 448–454.
- Kishimoto, H, Kojima, T, Watanabe, Y, Kagawa, S, Fujiwara, T, Uno, F *et al.* (2006). *In vivo* imaging of lymph node metastasis with telomerase-specific replication-selective adenovirus. *Nat Med* **12**: 1213–1219.
- Chen, CZ, Li, L, Lodish, HF and Bartel, DP (2004). MicroRNAs modulate hematopoietic lineage differentiation. *Science* **303**: 83–86.
- Sieuwerts, AM, Mostert, B, Bolt-de Vries, J, Peeters, D, de Jongh, FE, Stouthard, JM *et al.* (2011). mRNA and microRNA expression profiles in circulating tumor cells and primary tumors of metastatic breast cancer patients. *Clin Cancer Res* **17**: 3600–3618.
- Vincent, T, Neve, EP, Johnson, JR, Kukalev, A, Rojo, F, Albanell, J *et al.* (2009). A SNAIL1-SMAD3/4 transcriptional repressor complex promotes TGF- $\beta$  mediated epithelial-mesenchymal transition. *Nat Cell Biol* **11**: 943–950.

- Anders, M, Vieth, M, Röcken, C, Ebert, M, Pross, M, Gretschel, S *et al.* (2009). Loss of the coxsackie and adenovirus receptor contributes to gastric cancer progression. *Br J Cancer* **100**: 352–359.
- Yokobori, T, Iinuma, H, Shimamura, T, Imoto, S, Sugimachi, K, Ishii, H *et al.* (2013). Platin3 is a novel marker for circulating tumor cells undergoing the epithelial-mesenchymal transition and is associated with colorectal cancer prognosis. *Cancer Res* **73**: 2059–2069.
- Gaggar, A, Shayakhmetov, DM and Lieber, A (2003). CD46 is a cellular receptor for group B adenoviruses. *Nat Med* **9**: 1408–1412.
- Björge, L, Hakulinen, J, Wahlström, T, Matre, R and Meri, S (1997). Complement-regulatory proteins in ovarian malignancies. *Int J Cancer* **70**: 14–25.
- Varela, JC, Atkinson, C, Woolson, R, Keane, TE and Tomlinson, S (2008). Upregulated expression of complement inhibitory proteins on bladder cancer cells and anti-MUC1 antibody immune selection. *Int J Cancer* **123**: 1357–1363.
- Mizuguchi, H, Xu, ZL, Sakurai, F, Kawabata, K, Yamaguchi, T and Hayakawa, T (2005). Efficient regulation of gene expression using self-contained fiber-modified adenovirus vectors containing the tet-off system. *J Control Release* **110**: 202–211.
- Sakurai, F, Kawabata, K, Yamaguchi, T, Hayakawa, T and Mizuguchi, H (2005). Optimization of adenovirus serotype 35 vectors for efficient transduction in human hematopoietic progenitors: comparison of promoter activities. *Gene Ther* **12**: 1424–1433.
- Hashimoto, Y, Watanabe, Y, Shirakiya, Y, Uno, F, Kagawa, S, Kawamura, H *et al.* (2008). Establishment of biological and pharmacokinetic assays of telomerase-specific replication-selective adenovirus. *Cancer Sci* **99**: 385–390.
- Sakurai, F, Akitomo, K, Kawabata, K, Hayakawa, T and Mizuguchi, H (2007). Downregulation of human CD46 by adenovirus serotype 35 vectors. *Gene Ther* **14**: 912–919.
- Friedlander, TW, Ngo, VT, Dong, H, Premasekharan, G, Weinberg, V, Doty, S *et al.* (2014). Detection and characterization of invasive circulating tumor cells derived from men with metastatic castration-resistant prostate cancer. *Int J Cancer* **134**: 2284–2293.
- Li, YM, Xu, SC, Li, J, Han, KQ, Pi, HF, Zheng, L *et al.* (2013). Epithelial-mesenchymal transition markers expressed in circulating tumor cells in hepatocellular carcinoma patients with different stages of disease. *Cell Death Dis* **4**: e831.
- Yu, M, Bardia, A, Wittner, BS, Stott, SL, Smas, ME, Ting, DT *et al.* (2013). Circulating breast tumor cells exhibit dynamic changes in epithelial and mesenchymal composition. *Science* **339**: 580–584.
- Nadal, R, Ortega, FG, Salido, M, Lorente, JA, Rodríguez-Rivera, M, Delgado-Rodríguez, M *et al.* (2013). CD133 expression in circulating tumor cells from breast cancer patients: potential role in resistance to chemotherapy. *Int J Cancer* **133**: 2398–2407.
- Kasimir-Bauer, S, Hoffmann, O, Wallwiener, D, Kimmig, R and Fehm, T (2012). Expression of stem cell and epithelial-mesenchymal transition markers in primary breast cancer patients with circulating tumor cells. *Breast Cancer Res* **14**: R15.
- Baccelli, I, Schneeweiss, A, Riethdorf, S, Stenzinger, A, Schillert, A, Vogel, V *et al.* (2013). Identification of a population of blood circulating tumor cells from breast cancer patients that initiates metastasis in a xenograft assay. *Nat Biotechnol* **31**: 539–544.
- Al-Hajj, M, Wicha, MS, Benito-Hernandez, A, Morrison, SJ and Clarke, MF (2003). Prospective identification of tumorigenic breast cancer cells. *Proc Natl Acad Sci USA* **100**: 3983–3988.
- Dorsey, JF, Kao, GD, MacArthur, KM, Ju, M, Steinmetz, D, Wileyto, EP *et al.* (2015). Tracking viable circulating tumor cells (CTCs) in the peripheral blood of non-small cell lung cancer (NSCLC) patients undergoing definitive radiation therapy: pilot study results. *Cancer* **121**: 139–149.
- Lou, J, Ben, S, Yang, G, Liang, X, Wang, X, Ni, S *et al.* (2013). Quantification of rare circulating tumor cells in non-small cell lung cancer by ligand-targeted PCR. *PLoS One* **8**: e80458.
- Huang, S, Endo, RI and Nemerow, GR (1995). Upregulation of integrins alpha v beta 3 and alpha v beta 5 on human monocytes and T lymphocytes facilitates adenovirus-mediated gene delivery. *J Virol* **69**: 2257–2263.
- Leon, RP, Hedlund, T, Meech, SJ, Li, S, Schaack, J, Hunger, SP *et al.* (1998). Adenoviral-mediated gene transfer in lymphocytes. *Proc Natl Acad Sci USA* **95**: 13159–13164.
- Demirci, U, Coskun, U, Sancak, B, Ozturk, B, Bahar, B, Benekli, M *et al.* (2009). Serum granulocyte macrophage-colony stimulating factor: a tumor marker in colorectal carcinoma? *Asian Pac J Cancer Prev* **10**: 1021–1024.
- Vasilades, G, Kopanakis, N, Vasiloglou, M, Zografos, G, Margaritis, H, Masselou, K *et al.* (2012). Role of the hematopoietic cytokines SCF, IL-3, GM-CSF and M-CSF in the diagnosis of pancreatic and ampullary cancer. *Int J Biol Markers* **27**: e186–e194.
- Weng, NP, Levine, BL, June, CH and Hodes, RJ (1996). Regulated expression of telomerase activity in human T lymphocyte development and activation. *J Exp Med* **183**: 2471–2479.
- Igarashi, H and Sakaguchi, N (1997). Telomerase activity is induced in human peripheral B lymphocytes by the stimulation to antigen receptor. *Blood* **89**: 1299–1307.
- Wang, H, Li, ZY, Liu, Y, Persson, J, Beyer, I, Möller, T *et al.* (2011). Desmoglein 2 is a receptor for adenovirus serotypes 3, 7, 11 and 14. *Nat Med* **17**: 96–104.
- Chen, YS, Mathias, RA, Mathivanan, S, Kapp, EA, Moritz, RL, Zhu, HJ *et al.* (2011). Proteomics profiling of Madin-Darby canine kidney plasma membranes reveals Wnt-5a involvement during oncogenic H-Ras/TGF- $\beta$ -mediated epithelial-mesenchymal transition. *Mol Cell Proteomics* **10**: M110.001131.

42. Koizumi, N, Mizuguchi, H, Utoguchi, N, Watanabe, Y and Hayakawa, T (2003). Generation of fiber-modified adenovirus vectors containing heterologous peptides in both the HI loop and C terminus of the fiber knob. *J Gene Med* **5**: 267–276.
43. Dmitriev, I, Krasnykh, V, Miller, CR, Wang, M, Kashentseva, E, Mikheeva, G *et al.* (1998). An adenovirus vector with genetically modified fibers demonstrates expanded tropism via utilization of a coxsackievirus and adenovirus receptor-independent cell entry mechanism. *J Virol* **72**: 9706–9713.
44. Wickham, TJ, Tzeng, E, Shears, LL 2nd, Roelvink, PW, Li, Y, Lee, GM *et al.* (1997). Increased *in vitro* and *in vivo* gene transfer by adenovirus vectors containing chimeric fiber proteins. *J Virol* **71**: 8221–8229.
45. Lo, SL, Thike, AA, Tan, SY, Lim, TK, Tan, IB, Choo, SP *et al.* (2011). Expression of heparan sulfate in gastric carcinoma and its correlation with clinicopathological features and patient survival. *J Clin Pathol* **64**: 153–158.
46. Shinyo, Y, Kodama, J, Hasengaowa, Kusumoto, T and Hiramatsu, Y (2005). Loss of cell-surface heparan sulfate expression in both cervical intraepithelial neoplasm and invasive cervical cancer. *Gynecol Oncol* **96**: 776–783.
47. Smirnov, DA, Zwegitzig, DR, Foulk, BW, Miller, MC, Doyle, GV, Pienta, KJ *et al.* (2005). Global gene expression profiling of circulating tumor cells. *Cancer Res* **65**: 4993–4997.
48. Merkerova, M, Belickova, M and Bruchova, H (2008). Differential expression of microRNAs in hematopoietic cell lineages. *Eur J Haematol* **81**: 304–310.
49. Brown, BD, Venneri, MA, Zingale, A, Sergi, L and Naldini, L (2006). Endogenous microRNA regulation suppresses transgene expression in hematopoietic lineages and enables stable gene transfer. *Nat Med* **12**: 585–591.
50. Brown, BD, Gentner, B, Cantore, A, Colleoni, S, Amendola, M, Zingale, A *et al.* (2007). Endogenous microRNA can be broadly exploited to regulate transgene expression according to tissue, lineage and differentiation state. *Nat Biotechnol* **25**: 1457–1467.
51. Huang, B, Zhao, J, Lei, Z, Shen, S, Li, D, Shen, GX *et al.* (2009). miR-142-3p restricts cAMP production in CD4<sup>+</sup>CD25<sup>-</sup> T cells and CD4<sup>+</sup>CD25<sup>+</sup> TREG cells by targeting AC9 mRNA. *EMBO Rep* **10**: 180–185.
52. Ding, S, Liang, Y, Zhao, M, Liang, G, Long, H, Zhao, S *et al.* (2012). Decreased microRNA-142-3p/5p expression causes CD4<sup>+</sup> T cell activation and B cell hyperstimulation in systemic lupus erythematosus. *Arthritis Rheum* **64**: 2953–2963.
53. MacKenzie, TN, Mujumdar, N, Banerjee, S, Sangwan, V, Sarver, A, Vickers, S *et al.* (2013). Triptolide induces the expression of miR-142-3p: a negative regulator of heat shock protein 70 and pancreatic cancer cell proliferation. *Mol Cancer Ther* **12**: 1266–1275.
54. Kawashima, T, Kagawa, S, Kobayashi, N, Shirakiya, Y, Umeoka, T, Teraishi, F *et al.* (2004). Telomerase-specific replication-selective virotherapy for human cancer. *Clin Cancer Res* **10**(1 Pt 1): 285–292.
55. Mizuguchi, H and Kay, MA (1999). A simple method for constructing E1- and E1/E4-deleted recombinant adenoviral vectors. *Hum Gene Ther* **10**: 2013–2017.
56. Sakurai, F, Mizuguchi, H and Hayakawa, T (2003). Efficient gene transfer into human CD34<sup>+</sup> cells by an adenovirus type 35 vector. *Gene Ther* **10**: 1041–1048.
57. Mizuguchi, H, Kay, MA and Hayakawa, T (2001). *In vitro* ligation-based cloning of foreign DNAs into the E3 and E1 deletion regions for generation of recombinant adenovirus vectors. *Biotechniques* **30**: 1112–4, 1116.
58. Mizuguchi, H, Sasaki, T, Kawabata, K, Sakurai, F and Hayakawa, T (2005). Fiber-modified adenovirus vectors mediate efficient gene transfer into undifferentiated and adipogenic-differentiated human mesenchymal stem cells. *Biochem Biophys Res Commun* **332**: 1101–1106.



This work is licensed under a Creative Commons Attribution-NonCommercial-ShareAlike 4.0 International License. The images or other third party material in this article are included in the article's Creative Commons license, unless indicated otherwise in the credit line; if the material is not included under the Creative Commons license, users will need to obtain permission from the license holder to reproduce the material. To view a copy of this license, visit <http://creativecommons.org/licenses/by-nc-sa/4.0/>

Supplementary Information accompanies this paper on the *Molecular Therapy—Methods & Clinical Development* website (<http://www.nature.com/mtm>)